

UCLA

UCLA Previously Published Works

Title

Pile pinning and interaction of adjacent foundations during lateral spreading

Permalink

<https://escholarship.org/uc/item/1h04n0j9>

Journal

DFI Journal, 9(2)

ISSN

1937-5247

Authors

Turner, BJ
Brandenberg, SJ

Publication Date

2015-10-01

DOI

10.1179/1937525515Y.0000000009

Peer reviewed

This is the author's final version of the manuscript. The typeset version is under copyright, and can be downloaded from the following URL:

<http://www.tandfonline.com/doi/full/10.1179/1937525515Y.00000000009>

PILE PINNING AND INTERACTION OF ADJACENT FOUNDATIONS DURING LATERAL SPREADING

Benjamin J. Turner, Ph.D. Candidate, Dept. of Civil & Environmental Engineering, University of California, Los Angeles, bjturner@ucla.edu (corresponding author)

Scott J. Brandenburg, Professor and Vice Chair, Dept. of Civil & Environmental Engineering, University of California, Los Angeles

Abstract

Studies recently conducted by the authors and others have demonstrated that relatively simple equivalent-static analysis procedures can adequately predict the response of bridge foundations to lateral spreading for design purposes assuming that the lateral spreading displacement demand is known or can be estimated. However, an important aspect of the analysis that remains to be addressed is how to account for the restraining force provided by foundations when the laterally-spreading ground does not have a finite, measurable out-of-plane width. This study addresses this problem in the context of two parallel, adjacent bridges crossing the Colorado River in Mexico that were subjected to a broad field of laterally-spreading ground during the 2010 **M** 7.2 El Mayor-Cucapah earthquake. Two-dimensional finite element analyses are used to quantify the influence that the presence of each bridge had on the lateral spreading demand for the opposite bridge. The results show that the relatively stiff foundations of the first bridge provided a “shielding” effect to the second bridge, significantly reducing the demand compared to the magnitude of the free-field lateral spreading observed at the site.

Introduction

Liquefaction-induced lateral spreading has been a major cause of damage to bridges and waterfront infrastructure in past earthquakes (Idriss and Boulanger 2008). The underlying mechanics of the lateral spreading phenomenon are difficult to capture fully during foundation design, owing to the complexity of the phenomenon itself and the challenges associated with specifying accurate constitutive model parameters and executing dynamic numerical analyses. Rather, foundation designers desire simple yet effective equivalent-static analysis tools for addressing seismic issues such as lateral spreading on routine projects.

A recent set of guidelines published by the Pacific Earthquake Engineering Research (PEER) Center (Ashford et al. 2011) establishes an equivalent-static analysis (ESA) approach for design of bridge foundations in laterally spreading ground. In the ESA approach, a profile of horizontal ground displacement is imposed on the free ends of p - y springs attached to a beam-on-nonlinear-Winkler-foundation (BNWF) model, and the resulting shear, moment, and displacement of the foundation can be used to evaluate performance criteria and inform the structural design. This functionality is already implemented in some commercial software packages that are used for design of deep foundations under lateral loading such as *LPILE* (Reese et al. 2005).

This paper focuses on (1) pinning effects that occur when the aerial extent of the lateral spread feature is inadequate to fully encompass the passive loading zone of influence, and (2) shielding effects that occur when one foundation interacts with a lateral spread feature to reduce demands on an adjacent foundation. We first establish clear definitions of pinning and shielding. We then describe a case history of adjacent bridges in Mexico (Turner et al. 2014) where pinning and

shielding occurred. Finally, we develop a procedure that combines two-dimensional finite element simulations with ESA procedures to quantify pinning and shielding effects.

Definitions of Pinning and Shielding

The so-called “pinning” phenomenon is sometimes misunderstood and must be clearly defined to avoid confusion and misuse. In this paper, pinning is defined as a reduction in demand on a foundation embedded in a lateral spread feature with finite aerial extent compared to the demand that would be mobilized in an infinite-extent lateral spread. In the context of a beam on nonlinear Winkler foundation (BNWF) analysis, lateral spreading demands are represented as displacements imposed on the free-ends of p - y elements attached to the piles. If the aerial extent of the spread feature is large enough to fully encompass the zone of influence of soil-pile interaction, the free-field soil displacement is the appropriate input for the free-ends of the p - y elements. However, if the aerial extent of the spread feature is smaller than the zone of influence, the displacement demand must be reduced to account for pinning effects. The zone of influence of the foundations is defined as the region over which ground displacements are less than the free-field displacement.

Lateral spreading soil displacements in the vicinity of stiff foundations are often observed to be smaller than those in the "free-field" at some distance away from the foundation during post-earthquake reconnaissance efforts. This is true for both finite-extent and essentially infinite-extent lateral spread features. It is tempting to conclude that pile pinning must be responsible for this reduction in soil displacement. However, a reduction in soil displacement in the vicinity of the foundation is not a sufficient condition to conclude that pinning has occurred. Whether pinning

occurred can only be determined by assessing whether a reduction in demands resulted from the finite aerial extent of the spread feature.

To further clarify the definition of pinning in the context of lateral spreading problems, consider the single pile in the lateral spread feature with large horizontal spatial extent in Figure 1a. Assume for illustrative purposes that the pile foundation is embedded in underlying stiff soil, and the strength and flexural stiffness of the foundation is sufficiently high to limit the foundation displacements to negligible amounts as the spreading soil flows around the foundation. At large distances beyond the zone of influence of the foundation, the soil will exhibit a free-field displacement profile. However, within the zone of influence of the foundation the soil displacement will be reduced, and immediately behind the center line of the pile the soil displacement will equal the foundation displacement. The free-field soil displacement is clearly the correct input to a BNWF model in this case because the zone of influence of soil-pile interaction is completely contained within the spread feature. Therefore, consideration of pinning effects is not warranted. However, the stiffness of the load-transfer relationship between the pile and spreading crust may be significantly softer for liquefied soil profiles than for non-liquefied profiles due to a loss of shear stress on the bottom of the nonliquefiable crust layer (Brandenberg et al. 2007).

Now consider the finite-length lateral spread in Figure 1b. (*Note:* the following terminology is adopted for the remainder of this paper—the length of the lateral spread is measured in the direction of free-field soil displacement, and its width is measured along the transverse direction, as shown in Figure 1b). The zone of influence of soil-foundation interaction in this case extends

to the upslope margin of the spread feature. Therefore, the areal extent of the spread feature influences the formation of the soil passive failure mechanism, thereby reducing demands imposed on the foundation elements. Pinning effects therefore should be considered for this problem.

Finally, consider the finite-length, finite-width approach embankment spreading against a pile-supported abutment in Figure 1c. For this case, the zone of influence for soil-foundation interaction is geometrically limited by both the length and width of the spread feature. Demand could therefore be appreciably lower compared with the demand that would be mobilized by an embankment extending significantly further in one direction, such as a levee parallel to a river. Pinning is therefore an important consideration. McGann and Arduino (2014) used 3-D finite element modeling to demonstrate through back-analysis of damage to the Mataquito River Bridge in Chile that the width of an approach embankment undergoing lateral spreading has a significant influence on abutment pile demands.

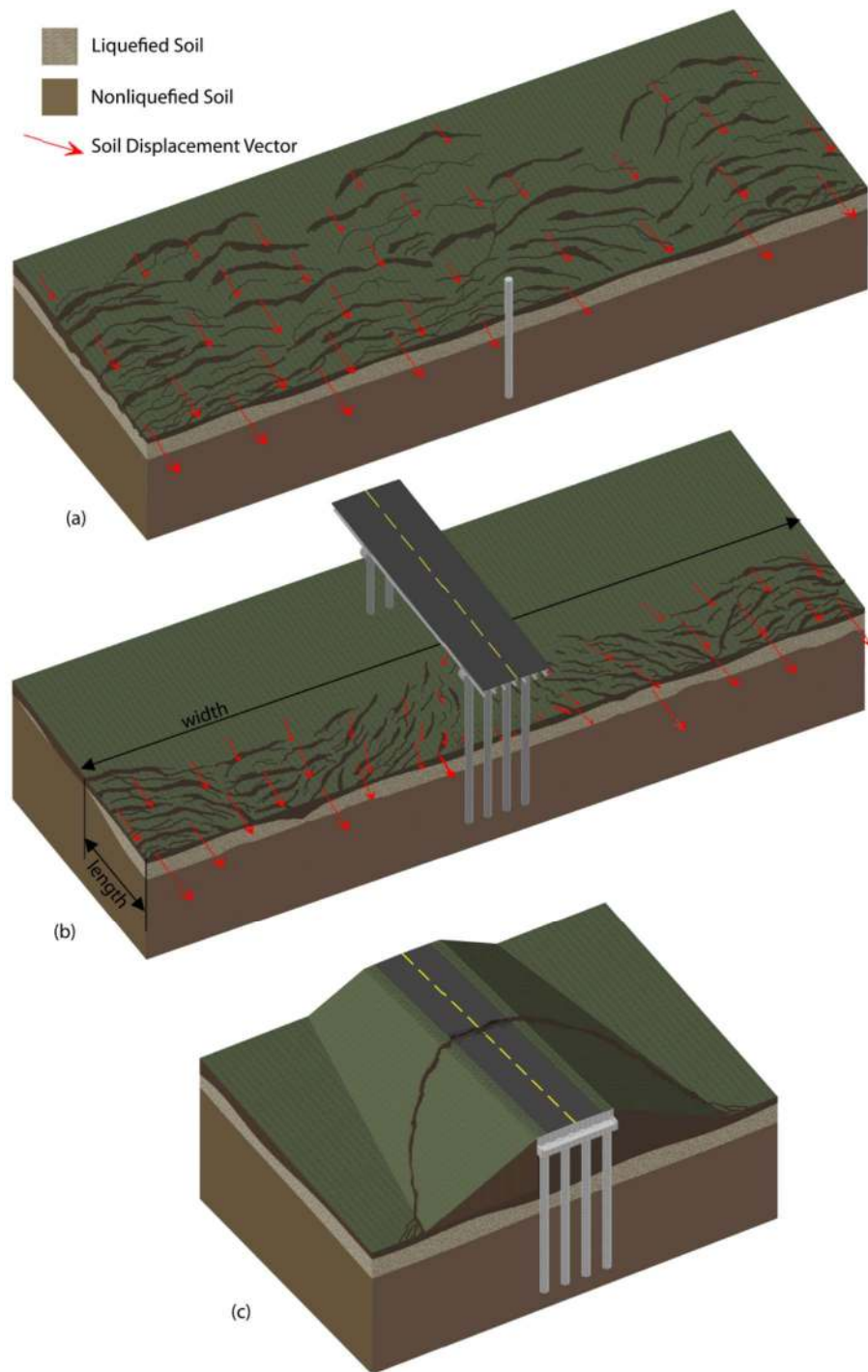


Figure 1: Three lateral spreading scenarios—(a) single pile subjected to broad field of lateral spreading, (b) pile group subjected to “short” lateral spread, and (c) laterally-spreading approach embankment resisted by abutment piles.

Methods have been proposed for analyzing the infinite-extent lateral spread cases in Figure 1a and the finite-width spread feature in Figure 1c. For infinite-extent lateral spreads (Figure 1a) the free-field displacement should be imposed, and can be crudely estimated using various procedures (e.g., Youd et al. 2002, Faris et al. 2006, Olson and Johnson 2008). Finite-width lateral spreads (Figure 1c) can be analyzed using an iterative procedure combining a pushover ESA analysis with limit equilibrium slope stability analyses with Newmark-type displacement estimates (e.g., Bray and Travarasrou 2007). This procedure results in a compatible slope displacement and foundation resistance for design (e.g., MCEER 2003, Boulanger et al. 2005). By contrast, pinning for “short” lateral spreads (Figure 1b) has not received adequate attention.

Shielding is defined as the reduction in demand imposed on one foundation component arising from soil-foundation interaction effects for an adjacent component. Imagine that the bridge in Figure 1b is adjacent to a second parallel bridge. Furthermore, assume that one of the bridges had foundations that are adequately stiff and strong to resist lateral spreading demands while the other bridge has weaker foundation elements that yield before mobilizing the passive resistance from the crust. In this case, the stronger foundation elements may exert a "shielding" effect that reduces lateral spreading demands on the weaker foundation elements. This is analogous to the shadowing effect for a closely-spaced group of piles, often accounted for with p -multipliers during analysis of laterally-loaded pile groups (e.g., Brown et al. 1987). The shielding effect for bridges in lateral spreads has not received adequate attention.

Case Study Background

The San Felipe Bridges cross the Colorado River about halfway between the USA/Mexico border and the Gulf of California. The crossing consists of a railroad bridge and a parallel highway bridge separated by about seven meters that span the river's roughly 200-m wide flood plain. The river has migrated to the west side of the incised flood plain, leaving a broad, gentle slope of relatively loose, liquefaction-prone deposits on the east bank. A site plan is presented in Figure 2.

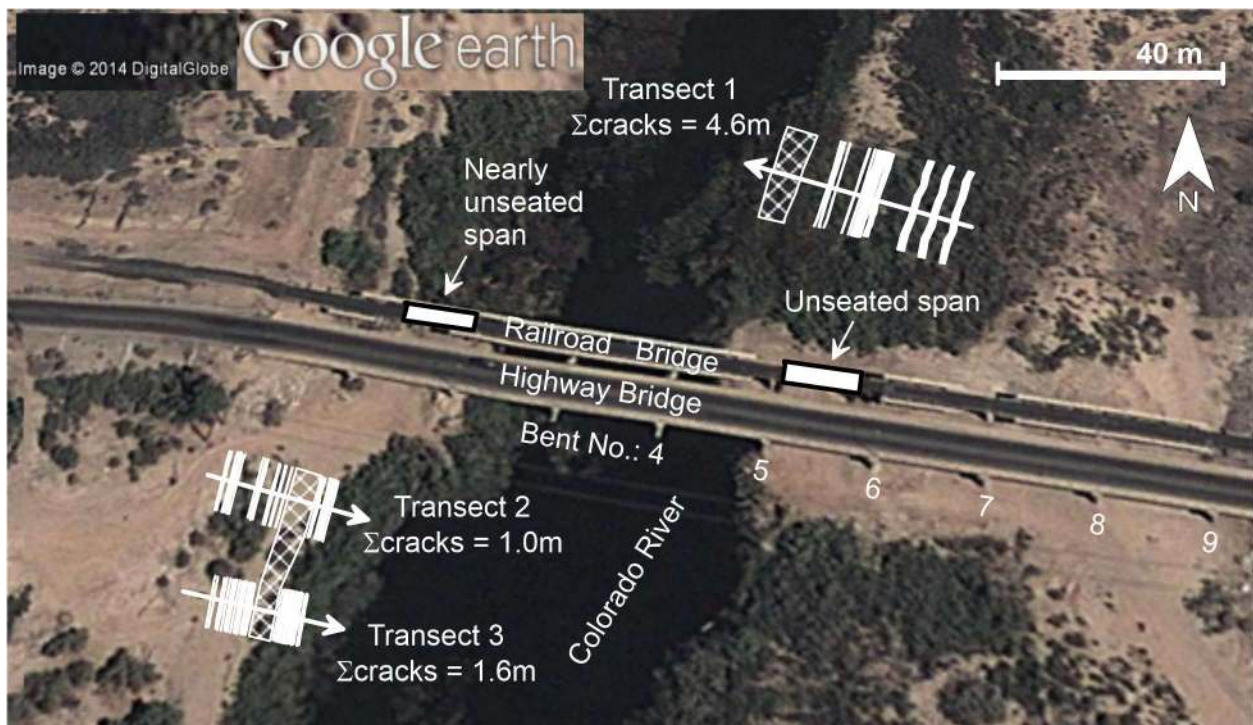


Figure 2: San Felipe Bridges site showing locations of structural damage and mapped ground failures following the 2010 El Mayor-Cucapah earthquake (after GEER, 2010). Google Earth base image 2014.

Both bridges are simply supported with 20-m long precast, prestressed concrete girders supporting their decks. Engineers from the regional transportation authority, *Secretaría de Comunicaciones y Transportes* (SCT) provided the construction plans of the highway bridge, built in 1999. Each bent is supported by four 1.2-m diameter extended-shaft columns that are continuous with drilled shafts of the same diameter to depths of up to 17 m below the ground surface. The longest shafts support

the spans over and immediately adjacent to the river crossing. Less is known about the railroad bridge, which is privately owned by Ferromex and was constructed in 1964 (EERI 2010). Each bent is supported by an oblong-shaped column atop a pile cap, which most likely connects a group of driven timber or steel piles. Construction documents were not available and the actual foundation details are unknown. However, Turner et al. (2014) showed that the observed behavior (described below) could be explained for a wide range of pile group configurations and pile material properties such as flexural stiffness and yield moment spanning an order of magnitude to represent timber, concrete, and steel piles. This is because the embedded pile cap attracted a large passive force from the crust soil, which was found in the ESA to cause yielding and subsequent collapse even when modeled with a foundation group considered representative of the upper bound strength and stiffness in terms of reasonable foundation types given the vintage and nature of railroad construction— a 4x7 group of 2-cm wall thickness, 30-cm diameter steel piles. Furthermore, we analyzed group configurations consisting of a single row of piles in the transverse direction and found that the lack of group overturning resistance provided by this configuration resulted in large predicted rotations that were contrary to the observed lack of rotation, so multiple rows in the longitudinal direction are most likely. These findings indicate that the railroad bridge bent behavior is relatively insensitive to the pile foundation details and is instead dominated by the magnitude of the lateral spreading displacement demand and the corresponding load imposed on the pile cap.

Teams from the Geotechnical Extreme Events Reconnaissance (GEER) Association and the Earthquake Engineering Research Institute (EERI) documented ground failures and structural damage following the 2010 earthquake (GEER 2010; EERI 2010). As shown in Figure 3, peak

lateral spreading displacement in the free-field to the north of the bridges was measured as approximately 4.6 m. While there is inherent spatial variability in the magnitude of free-field lateral spreading, this zone was observed to move relatively uniformly towards the river, and hence we used 4.6 m as an approximate representation of the free-field displacement in our subsequent analyses. A span of the railroad bridge adjacent to the east river bank unseated and collapsed as a result of translation of Bent 5 toward the river during lateral spreading (see Figure 3). The railroad bridge bent adjacent to the west bank also translated toward the river, stopping just short of causing a similar unseating collapse. The highway bridge suffered only moderate damage, including flexural cracking at the base of the Bent 5 columns as a result of the lateral spreading demand. Note in Figures 2 and 3 that Bent 5 of the railroad bridge and the highway bridge are directly adjacent to one another and located approximately the same distance from the east river bank.

The authors participated in a research study of the San Felipe Bridges as described in detail by Turner et al. (2014). A team from UCLA performed a series of cone penetration tests (CPT) and geophysical tests at the site in October of 2013 to characterize the subsurface. Our investigation was supplemented by boring logs and index tests results performed previously by SCT and Ferromex.



Figure 3: Bent 5 of railroad bridge (foreground) that translated towards river causing unseating collapse, and Bent 5 of highway bridge (background) following 2010 El Mayor-Cucapah earthquake. Photo J. Gingery/GEER (2010).

The stratigraphy in the vicinity of Bent 5 of the bridges, which was the focus of the lateral spreading analyses, generally consists of a 1.5-m thick crust of silty sand above the groundwater table underlain by interbedded layers of loose, liquefiable sand and medium dense to very dense

sand and silty sand. The fines content generally decreased with increasing depth. CPT performed adjacent to Bents 6 and 7 revealed the same stratigraphic pattern, except that penetration resistance increased with increasing distance from the river, indicating that the deposits nearest the river were likely younger and hence more prone to liquefaction. The thickness of the loose layers also decreased with increasing distance from the river. This pattern likely played a role in defining the margins of the lateral spreading that occurred during the 2010 earthquake.

We used the CPT and previous index test results to develop a profile of idealized stratigraphy and soil properties for the analyses. The estimated soil properties were used to develop p - y springs to represent the soil-structure interaction between the foundations and the ground, including the softened load-transfer behavior of the crust due to the underlying liquefied layers as described by Brandenberg et al. (2007). P - y springs were based on the API sand formulation (API 1993), and liquefied soil was represented using p - y springs reduced by a p -multiplier. The p -multiplier values were computed using the best-fit equation to multiple empirical studies presented in the California Department of Transportation lateral spreading guidelines (2013). Because the response of the bridges was dominated by the load transfer of the crust layer, the results were relatively insensitive to a range of p -multipliers considered for the liquefied layer. T - z and q - z springs were used to represent the pile axial stiffness to capture the overturning resistance provided by group interaction for the railroad bridge.

BNWF models of Bent 5 of each bridge were analyzed using the open-source finite element modeling platform *OpenSees* (McKenna and Fenves 2010). Structural modeling of the highway bridge was based on the member dimensions and material properties shown on the construction

plans and verified in the field; for the railroad bridge we measured member dimensions in the field and assumed typical ranges of concrete and steel material properties. The railroad bridge pile group was modelled explicitly to capture group interaction and overturning resistance effects due to multiple rows of piles in the lateral spreading direction; for the highway bridge a single extended-shaft column was modelled and considered representative of all four shafts within the single-row group. Formulation of the p -y springs that represent the passive load-transfer of the crust takes the extended-shaft column spacing and group geometry into consideration. Nonlinear structural behavior such as concrete cracking and steel yielding was captured via bilinear moment-curvature relationships.

The ESA procedure was found to capture the observed behavior of both bridges well. The difference in behavior is ultimately attributable to the lateral resistance of the highway bridge foundations being sufficient to resist the fully-mobilized passive pressure of the laterally spreading crust, whereas the lateral resistance of the railroad bridge was not sufficient to resist the crust load without yielding and undergoing large displacement. Complete results of the site investigation and analyses are presented in Turner et al. (2014).

Bent 5 of the railroad bridge was observed to have translated about 1 m based on measurements taken following the earthquake (Figure 3). From the ESA analyses, Bent 5 was predicted to undergo sufficient translation to cause an unseating collapse (about 0.85 m of movement was required) for imposed free-field lateral spreading displacements exceeding about 1 m. However, if the full free-field lateral spreading displacement of approximately 4.6 m was imposed, Bent 5 was predicted to displace about 4.1 m, which greatly exceeds the observed movement. A working

hypothesis is that shielding provided by the highway bridge is responsible for the translation of Bent 5 being less than predicted under free-field lateral spread demands. In addition, bents further away from the river bank (6, 7 etc.) would be predicted to undergo significant translation when subjected to the level of lateral spreading observed in the free-field at the respective distance from the bank, but they underwent no measureable displacement. We postulate that this better-than-predicted behavior arises from a combination of shielding provided by the highway bridge, and pinning resulting from the upslope extent of the lateral spread behind the bents being small relative to the highway bridge foundations' zone of influence.

This case study provides a unique opportunity to explore methods for quantifying the shielding effect, since the site is well characterized, free field lateral spreading displacements were measured, the performance of the bridges during the earthquake was well documented, and the ESA of the foundations under lateral spreading demand has already been performed.

Approach

The approach adopted to quantify shielding and pinning effects consists of two-dimensional finite element analyses (FEA) of a plan-view section of the domain combined with parameters obtained from the previously-performed ESA simulations. Although this is a 3-D problem, a 2-D simulation was adopted for simplicity. The FEA consisted of a 1-m thick horizontal slice of the crust (*i.e.*, the domain represents a plan-view of the system), and were conducted using the program *Phase2* by Rocscience (2013). The model included Bents 5, 6, and 7 of the highway bridge in the center of a 150-m wide by 60-m long domain. The domain is sufficiently large so that a free-field response occurs outside the zone of influence of the foundations. Bents further to the east (Bents 8, 9 etc.)

were not included since they are beyond the zone of observed lateral spreading in the free field, which extended about 50 m upslope from the east river bank. Bent 4 is not included in the model because it is located in the middle of the river channel; the lateral spread is assumed to have stopped shortly after entering the river from the east bank and likely did not interact with Bent 4. Bents of the railroad bridge were not included in the initial model so that the shielding effect provided by the highway bridge on the railroad bridge could be studied independently. In reality, the two bridge systems constitute an interacting system in which the railroad bridge may have also provided a shielding effect for the highway bridge. This effect is considered small in this case because the railroad bridge foundations were weaker and more flexible than those for the highway bridge. The interaction would be important for adjacent foundations with similar strength and stiffness.

The relationship between mobilized passive pressure and free-field displacement was obtained from the *OpenSees* ESA (Figure 4). The average horizontal stress was found to be 78 kPa with 4.6 m of free-field soil displacement, inducing a corresponding foundation displacement of 4.0 cm at the ground surface. This horizontal pressure represents a Rankine passive limit state corresponding to a friction angle of 35° . These results were used to define an elastic perfectly-plastic model for the crust soil in *Phase2* with uniform shear strength of 54 kPa such that the same passive limit state would be mobilized in the plain strain simulations. The perfectly-plastic behavior ensures that the soil cannot transfer additional load to the foundations once the passive limit state has been reached. Although the individual soil elements are modeled with a bilinear stress-strain relationship, the pile lateral response obtained from the simulations is nonlinear due to incremental shear failure of the soil elements. We acknowledge that the two-dimensional, plain strain analysis used here does not capture the three-dimensional boundary conditions of the lateral spreading

problem very well. The material properties for the two-dimensional analysis must be carefully selected so that the desired passive pressure is achieved.

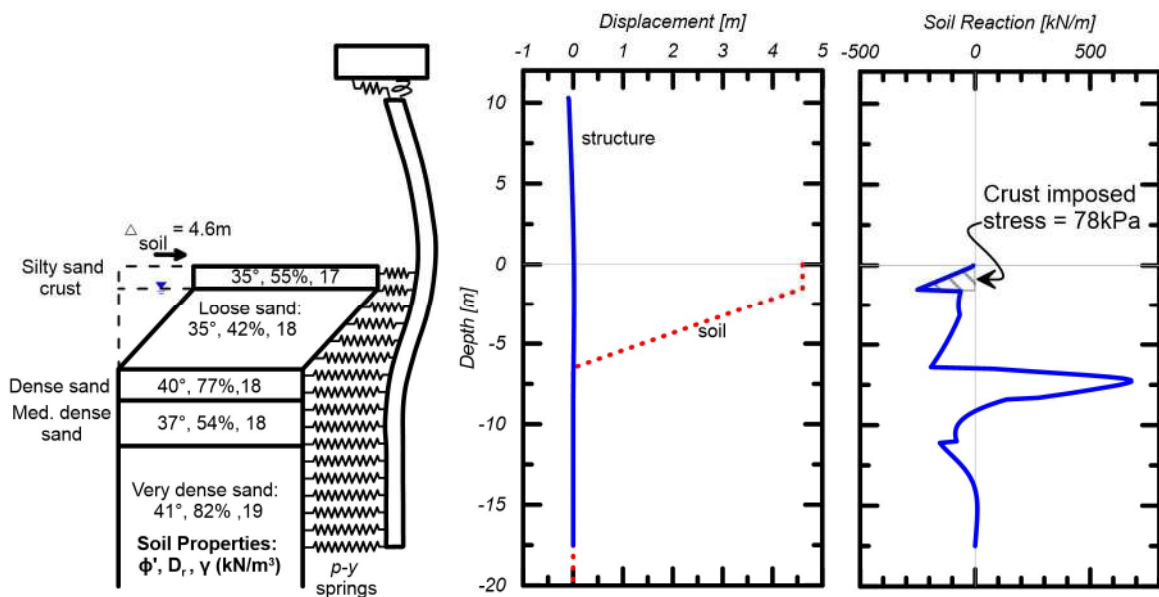


Figure 4: Equivalent-static analysis results. After Turner et al. (2014).

The lateral boundaries of the finite element domain were restrained against displacement in the x -direction (*i.e.*, the domain could not change width) and a uniform displacement of 4.6 m was imposed on the lateral boundaries in the y -direction (*i.e.*, towards the river) as shown in Figure 5. In reality there was a non-uniform gradient of displacement along the length of the lateral spread, though most of the soil displacement was accommodated by several large cracks approximately 40 meters upslope from the river. In other words, a block about 40 meters long displaced relatively uniformly towards the river. A uniform displacement imposed on the boundaries is therefore considered reasonable for this exercise.

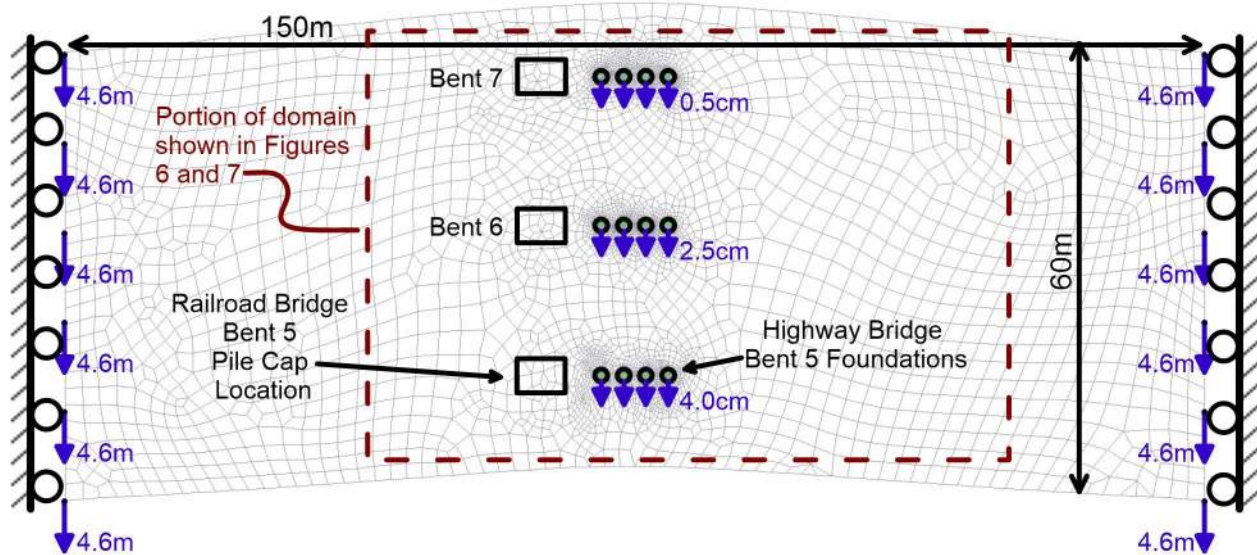


Figure 5: Finite element domain.

To determine the Young's modulus of the crust soil, the lateral boundaries of the domain were displaced 4.6 m and the Bent 5 foundations were displaced by the amount predicted from the ESA, 4.0 cm, as shown in Figure 5. Bents 6 and 7 of the highway bridge were initially held fixed against translation; the Young's modulus of the crust soil and displacement of Bents 6 and 7 were then adjusted until the average reaction force of the crust acting against the foundations of each bent and the corresponding displacement were in agreement with the ESA results as shown in Figure 6. A modulus of 875 kPa was found to provide a good match. This value is significantly less than the small-strain modulus for cohesionless soils under typical loading conditions, which can be attributed to the low confining pressure near the surface and large modulus reduction at high strain as well as the loss of shear resistance at the bottom of the spreading layer (Brandenberg et al. 2007). The results were found to be relatively insensitive to a range of Poisson's ratio between 0.2 and 0.35, typical for loose cohesionless soil (Bowles 1996). A small amount of tensile strength (5 kPa) was assigned to the soil to prevent excessive deformation for soil elements that yield in

tension. Foundation resistance provided by the railroad bridge was not included in the domain for the soil modulus calibration step. If the foundations of the secondary structure have comparable resistance to the primary structure, they should be included in the calibration step. Concrete drilled shafts were modeled in *Phase2* with an elastic material having a Young's modulus of 27 GPa and a Poisson's ratio of 0.2.

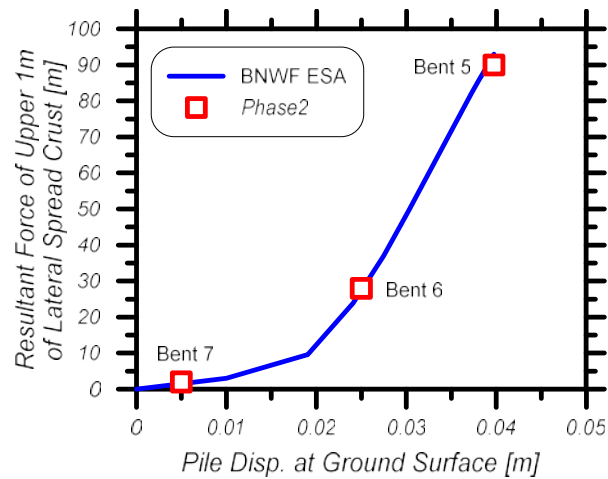


Figure 6: Highway bridge mobilized force-displacement results for soil property calibration step.

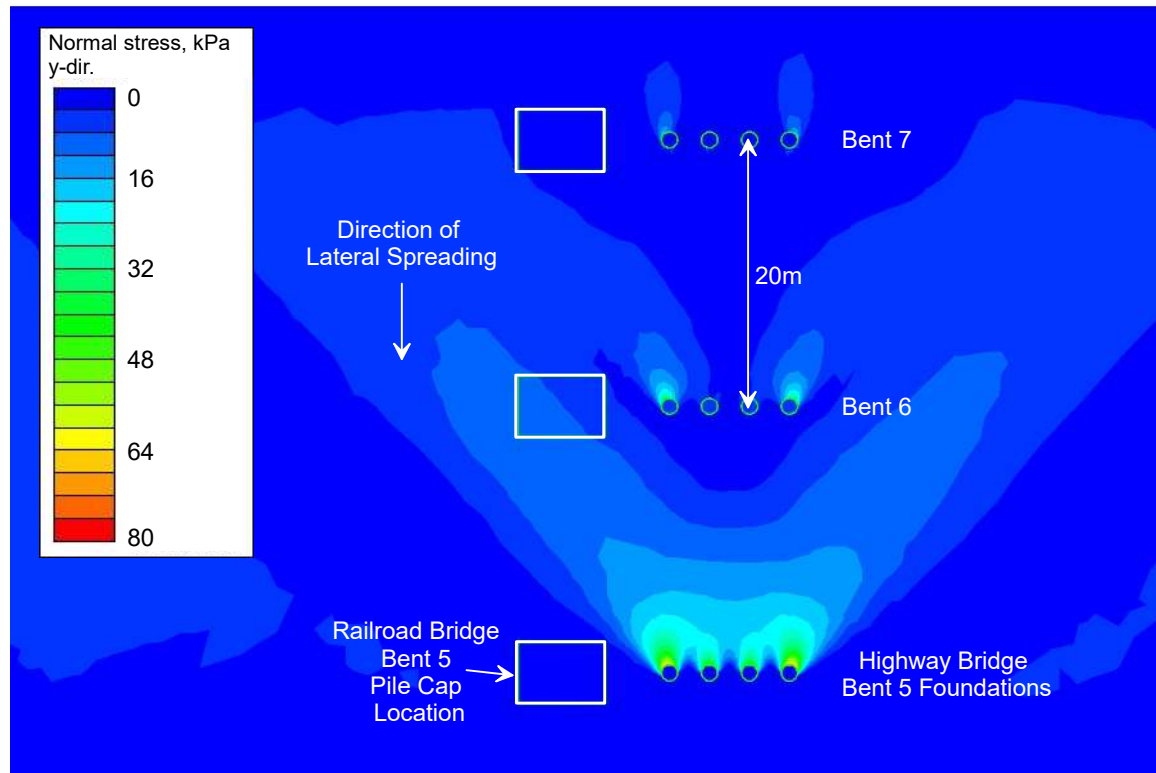


Figure 7: Results of *Phase2* simulations with 4.6 m of imposed free-field lateral spreading displacement, showing normal stress acting in direction of lateral spreading. Stress contours in kPa.

The steps followed to estimate the reduced demand at the location of a secondary structure due to shielding by the foundations of a primary structure were:

1. Performed ESA for the primary structure foundations using the free-field lateral spreading displacement to determine the average stress intensity acting on the foundations (Figure 4) and the corresponding foundation displacement versus soil reaction force relationship (Figure 6);
2. Developed finite element model of the crust layer, including foundations of the primary structure, and adjusted soil modulus and foundation displacement until soil reaction

force and foundation displacement are in agreement with the ESA results determined in step 1 (i.e., the “calibration step”—Figures 5, 6, and 7);

3. Determined reduction of free-field lateral spreading displacement at the location of the secondary structure foundations;
4. Performed ESA for secondary structure foundations using reduced lateral spreading displacement demand.

Results

Average predicted displacement towards the river at the location of Bent 5 of the railroad bridge was 1.36 m for an imposed free-field lateral spreading displacement of 4.6 m as shown in Figure 8. This represents a 70-percent reduction from the free-field lateral spreading demand. When the reduced demand is imposed on an ESA model of the bent, the bent is predicted to displace about 1.2 m, which induces unseating collapse of the span and agrees reasonably with the measured pier displacement of about 1 m.

Further studies were conducted to isolate the shielding effect in the transverse and longitudinal directions. A model that only included Bent 5 of the highway bridge (Bents 6 and 7 removed) provided a 68-percent reduction of the free-field displacement at the location of Bent 5 of the railroad bridge, which represents shielding only in the transverse direction. If the railroad bridge had been located an additional 15 m away from highway bridge, the predicted shielding effect would decrease to 45 percent. A model that only included Bents 6 and 7 of the highway bridge provided a 42-percent reduction for the railroad bridge Bent 5, which is primarily longitudinal shielding in the “downstream” lateral spreading direction. In the “upstream” shielding case, a

model that only included Bent 5 of the highway bridge provided a 87-percent reduction at the location of Bent 6 of the railroad bridge. It is also apparent that the highway bridge shielded itself, with the presence of Bents 6 and 7 reducing demand on Bent 5 by about 45 percent. These results demonstrate that longitudinal and transverse shielding effects are both significant and can be investigated separately.

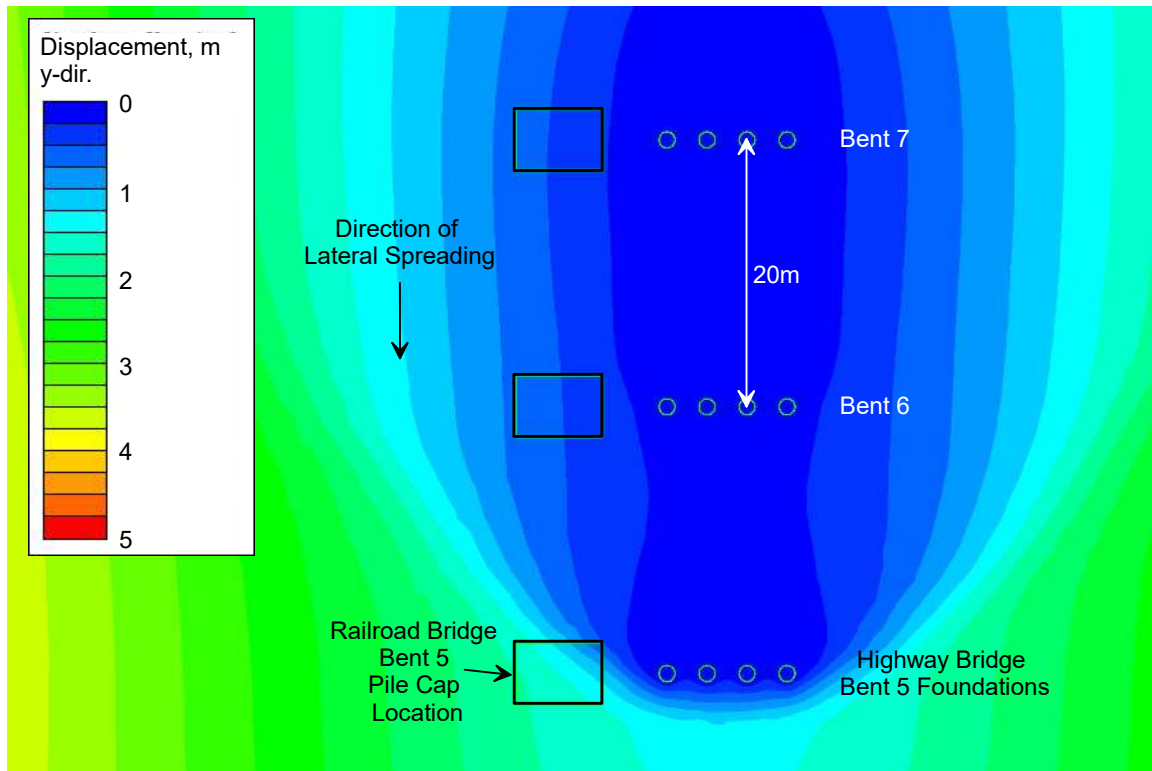


Figure 8: Displacement results (in meters) for finite element model including Bents 5, 6, and 7 of the highway bridge showing reduction in displacement at location of railroad bridge Bent 5 compared to free-field lateral spreading displacement of 4.6 m.

For bents of the railroad bridge further from the river bank (No.'s 6 and 7), the predicted reduced displacement demand still results in prediction of significant displacement during the ESA, about 0.4 m, which is contrary to the observed behavior. This can partially be explained by the uniform displacement gradient that was imposed on the model and the fact that the soil properties are different at these locations compared to the Bent 5 location, notably that the thickness of the

liquefiable layer decreases further from the river. For forward design cases, knowingly underestimating the shielding effect is a reasonable approach given the uncertain nature of estimating the magnitude and margins of lateral spreading.

In contrast to the shielding provided by the highway bridge, Bent 5 of the railroad bridge only provides an 8 to 10 percent reduction in the lateral spreading displacement demand at the location of Bent 5 of the highway bridge. Since the highway bridge foundations have sufficient strength and stiffness to resist the fully-mobilized passive pressure of the laterally spreading crust, the low shielding effect provided by the railroad bridge is of little consequence. Nonetheless, the analysis did correctly predict that the highway bridge shaft closest to the railroad bridge experienced slightly less demand than the furthest shaft which agrees with the observed gradient of residual rotations measured in the four columns of Bent 5 following the earthquake.

Influence of Lateral Spread Length

A separate issue, also missing from the literature, is the influence of the length of the lateral spread. Spread features that are “short” in length along the longitudinal axis of the bridge can be restrained more effectively by the bridge foundations than an equivalent-width lateral spread that extends upslope for a larger distance but undergoes the same free-field displacement. The zone of stress influence for loading conditions below that which is required to fully mobilize passive failure can be relatively large in lateral spread features because the low friction along the base of the spreading crust (i.e., at the interface with the liquefiable sand) results in horizontal pressures transferring further upslope than they otherwise would in a non-liquefied soil profile (e.g., Brandenburg et al. 2007). As a result, lateral spreading occurring a significant distance upslope from a foundation can

be “felt” by the foundation even when soil displacement at this location under non-liquefied conditions would have a negligible influence on the foundation. The aerial extent of the spread no longer has an influence when full passive pressures are mobilized in the soil, since the passive pressure limit state does not depend on the length of the spread feature, although the size of the passive wedge will still be larger than in a non-liquefaction case. An exception is when the passive wedge extends beyond the upslope extent of the spread feature, in which case a reduction in passive force would be anticipated relative to the case in which the entire passive wedge is contained within the spread feature.

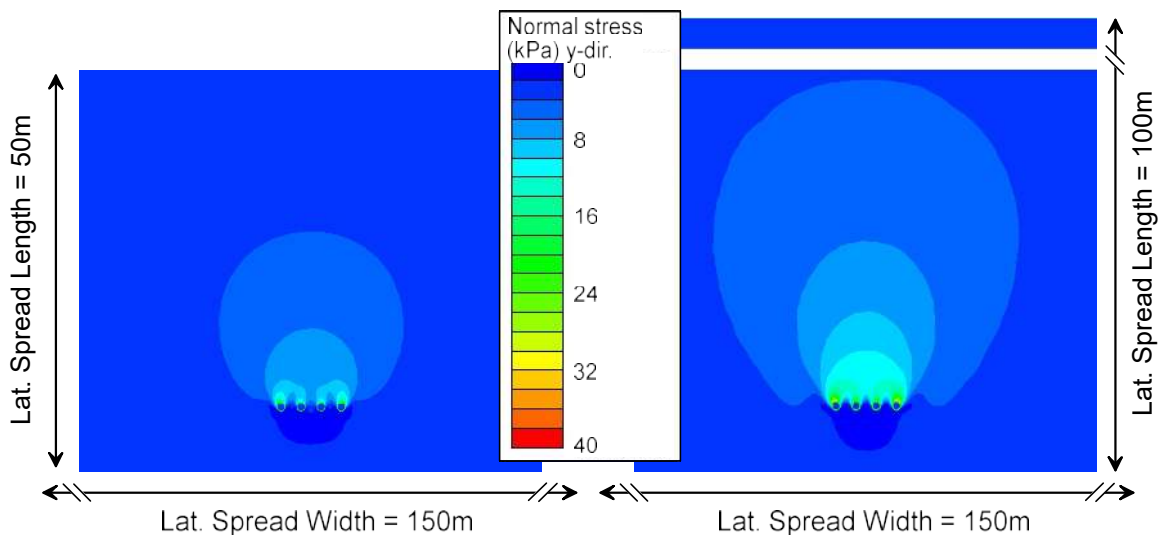


Figure 9: Influence of lateral spread length; only the length of the lateral spread is varied between the two cases.

For example, if the entire flood plain on the east bank liquefied and spread at the Mexico site (lateral spread length of approximately 100 m instead of 50 m), predicted pressures acting against the Bent 5 highway bridge foundations are about 40 percent higher when the free-field lateral spreading displacement is 0.5 m (less than the amount required to mobilize full passive pressure) as shown in Figure 9. This trend demonstrates that as the length of a lateral spread increases and

the foundation zone of influence becomes smaller relative to the aerial extent of the lateral spread, the appropriate demand for an ESA approaches the free-field displacement.

Conclusions

A procedure combining the results of equivalent static analysis (ESA) procedures for estimating foundation demand under lateral spreading loading with two-dimensional finite element analyses of the laterally spreading crust layer was utilized to study pinning and shielding effects for pile foundations. For foundation groups subjected to very broad lateral spreads in which the zone of influence is entirely contained within the spread feature, the appropriate input displacement for ESA is the free-field displacement. For pile groups subjected to “short” lateral spreads in which the zone of influence of the foundations extends beyond the aerial extent of the lateral spread, demands on the foundation are reduced relative to inputting a free-field displacement profile on the free-ends of the p - y elements in an ESA.

This procedure has been applied to a case study of two adjacent bridges that were subjected to lateral spreading during the 2010 El Mayor-Cucapah earthquake. Lateral spreading demand at the location of the railroad bridge foundations that were damaged during the earthquake was predicted to be reduced by about 70 percent compared to the free-field displacement measured at the same distance upslope from the river bank. The results of ESA performed using this reduced displacement closely match the observed bridge performance, whereas ESA performed using the free-field displacement over-predicts foundation displacement.

Since the resistance provided by the foundation being investigated is not included in the proposed model, the displacement reduction may be underestimated for cases when the resistance of the individual foundation represents a significant portion of the total foundation group resistance. This would be most significant for cases where few large-diameter shafts are used and the resistance against lateral spreading provided by a single shaft is significant. In this case, all the foundations providing significant resistance should be included in the soil modulus calibration step. For the case study considered herein, the resistance provided by the railroad bridge foundations was small relative to the resistance provided by the highway bridge foundations.

A limitation of the proposed method as described herein is that only a single layer is considered to dominate the load-transfer behavior between the lateral spread and the foundations, in this case the nonliquefied crust. If multiple nonliquefied layers exist between liquefied layers and undergo significant displacement relative to the foundations, it may not be possible to adequately simplify the behavior to two dimensions. Nonetheless, in many lateral spreading scenarios a single layer of nonliquefied crust overlying liquefied soil does impose the majority of the demand on the foundations, and the two-dimensional approach may be adequate.

The findings of this study show that the length and width of the lateral spread feature relative to the size of the foundation zone of influence affects the load imposed on the foundations by the moving soil. The traditional pinning approach does not account for these effects well when applied to mid-span bents. For example, Kato et al. (2014) applied the pinning approach to back-analysis of three bridges and found that the observed performance was not matched in all cases, concluding that the three-dimensional geometry of the problem has a clear influence on the pile response.

The analysis method proposed herein can be used to assess the appropriate demand for foundation groups. The free-field displacement should be applied for mono-foundations or in very broad lateral spreads, including softened p - y behavior to account for loss of shear resistance at the bottom of the spreading layer following recommendations by Brandenberg et al. (2007). Additionally, the sensitivity of the two-dimensional analysis results to changes in aerial extent and magnitude of free-field displacement can provide insight to the potential consequences of actual lateral spreading displacements exceeding the estimated amount.

Foundation engineers are cautioned to carefully consider the boundary conditions of each individual project and whether or not two-dimensional analyses can adequately capture the real system behavior. It is important to recognize that the results of the procedure presented here are approximate and should not be treated as a guaranteed representation of actual system performance. For high-value or critical projects, the results of two-dimensional analyses could be used to justify whether or not more sophisticated analyses are warranted.

Acknowledgments

Funding for the San Felipito Bridges study was provided by the PEER center. The assistance of SCT engineers and Raul Flores Berrones in obtaining design and construction documents for the bridges is greatly appreciated, as is the assistance of the UCLA/UC Davis field and laboratory team that conducted the 2013 site investigation.

References

- American Petroleum Institute (API), 1993. Recommended practice for planning, design, and constructing fixed offshore platforms, API Report 2A-WSD, 20th Edition, API Publishing Services, Washington DC.
- Ashford, SA, Boulanger, RW, and Brandenburg, SJ, 2011. Recommended design practice for pile foundations in laterally spreading ground. PEER report 2011/04, Pacific Earthquake Engineering Research Center, University of California, Berkeley. 43 p.
- Boulanger, RW, Chang, D., Gulerce, U., Brandenburg, SJ, and Kutter, BL (2005). Evaluating pile pinning effects on abutments over liquefied ground. Seismic Performance and Simulation of Pile Foundations in Liquefied and Laterally Spreading Ground, ASCE Geotechnical Special Publication No. 145, RW Boulanger and K. Tokimatsu, eds., pp. 306-318.
- Bowles, JE (1996). Foundation analysis and design—5th edition. McGraw-Hill Book Co., New York. 1241 p.
- Brandenburg, SJ, Boulanger, RW, Kutter, BL, and Chang, D. (2007). Liquefaction-induced softening of load transfer between pile groups and laterally spreading crusts. J. of Geotech. and Geoenviron. Eng., ASCE, 133(1): 91–103.
- Bray, JD, and Travasarou, T., 2007. Simplified procedure for estimating earthquake-induced deviatoric slope displacements. J. of Geotech. and Geoenviron. Eng., ASCE, 130(12): 1314-1340.
- Brown, DA, Reese, LC, and O'Neill, MW, 1987. Cyclic lateral loading of a large-scale pile group. J. of Geotech. Eng., ASCE, 113(11): 1326-1343.
- Caltrans (2013). Guidelines on Foundation Loading and Deformation due to Liquefaction Induced Lateral Spreading, California Department of Transportation, Sacramento, CA.
- Earthquake Engineering Research Institute (EERI), 2010. Meneses, J. (editor). The El Mayor Cucapah, Baja California earthquake, April 4, 2010. EERI Reconnaissance Report 2010-02, available: <http://www.eeri.org>.
- Faris, AT, Seed, RB, Kayen, RE, and Wu, J., (2006). A semi-empirical model for the estimation of maximum horizontal displacement due to liquefaction-induced lateral spreading. Proc. 8th National Conference on Earthquake Engineering, Earthquake Engineering Research Institute, San Francisco, CA.
- Geotechnical Extreme Event Reconnaissance (GEER), 2010. Stewart, JP, Brandenburg SJ (editors). Preliminary report on seismological and geotechnical engineering aspects of the April 4 2010 Mw 7.2 El Mayor-Cucapah (Mexico) Earthquake”, Report No. GEER-023, available: <http://www.geerassociation.org/>

- Kato, K., Gonzales, D., Ledezma, C., and Ashford, S. (2014). Analysis of pile foundations affected by liquefaction and lateral spreading with pinning effect during the 2010 Maule Chile Earthquake. Proc. 10th National Conference on Earthquake Engineering, Earthquake Engineering Research Institute, Anchorage, AK.
- Idriss, IM, and Boulanger, RW, 2008. Soil liquefaction during earthquakes, Monograph MNO-12, Earthquake Engineering Research Institute, Oakland, CA. 237 p.
- MCEER/ATC-49 (2003). "Recommended LRFD guidelines for the seismic design of highway bridges." Multidisciplinary Center for Earthquake Engineering Research, Report No. MCEER-03-SP03.
- McGann, C. and Arduino, P. (2014). Numerical assessment of three-dimensional foundation pinning effects during lateral spreading at the Mataquito River Bridge. J. Geotech. Geoenviron. Eng., ASCE, 140(8), 10 p.
- McKenna F.T., Scott, M.H., and Fenves, G.L. (2010). Nonlinear finite-element analysis software architecture using object composition. J. of Computing in Civil Eng., ASCE, 24(1): 95-107.
- Olson, S. and Johnson, C. (2008). Analyzing liquefaction-induced lateral spreads using strength ratios. J. Geotech. Geoenviron. Eng., ASCE, 134(8): 1035–1049.
- Reese, LC, Wang, ST, Isenhower, WM, Arrelaga, JA, and Hendrix, JA, 2005. LPILE plus version 5.0. Ensoft, Inc., Austin, TX.
- Rocscience, 2013. Phase2. Version 8.016, Rocscience Inc., Toronto, Can.
- Turner, B, Brandenburg, SJ, and Stewart, JP, 2014. Evaluation of collapse and non-collapse of parallel bridges affected by liquefaction and lateral spreading. PEER report 2014/10, Pacific Earthquake Engineering Research Center, University of California, Berkeley. 94 p.
- Youd, TL, Hansen, CM, and Bartlett, SF (2002). Revised multi-linear regression equations for prediction of lateral spread displacement. J. Geotech. Geoenviron. Eng., ASCE, 128(12), 1007-1017.

List of Figure Captions:

1. Three lateral spreading scenarios—(a) single pile subjected to broad field of lateral spreading, (b) pile group subjected to “short” lateral spread, and (c) laterally-spreading approach embankment resisted by abutment piles.
2. San Felipe Bridges site showing locations of structural damage and mapped ground failures following the 2010 El Mayor-Cucapah earthquake (after GEER, 2010). Google Earth base image 2014.
3. Bent 5 of railroad bridge (foreground) that translated towards river causing unseating collapse, and Bent 5 of highway bridge (background) following 2010 El Mayor-Cucapah earthquake. Photo J. Gingery/GEER (2010).
4. Equivalent-static analysis results. After Turner et al. (2014).
5. Finite element domain.
6. Highway bridge mobilized force-displacement results for soil property calibration step.
7. Results of Bent 5 finite element simulations with 4.6 m of imposed free-field lateral spreading displacement, showing normal stress acting in direction of lateral spreading. Stress contours in kPa.
8. Displacement results (in meters) for finite element model including Bents 5, 6, and 7 of the highway bridge showing reduction in displacement at location of railroad bridge Bent 5 compared to free-field lateral spreading displacement of 4.6 m.
9. Influence of lateral spread length; only the length of the lateral spread is varied between the two cases.